Journal of Inclusion Phenomena and Molecular Recognition in Chemistry **28:** 63–78, 1997.

Interaction of the *t*-butylcalix[4]arene Anion with Ammonium Cations in Acetonitrile: Host–Guest Complexes or *exo* Counterions? A Molecular Dynamics Investigation

F. FRATERNALI and G. WIPFF*
Laboratoire MSM, URA 422 CNRS, Institut de Chimie, 4, rue B. Pascal, 67 000 Strasbourg, France.

(Received: 15 August 1996; in final form: 14 November 1996)

Abstract. We report a theoretical study of the NR_4^+ salts (R = H; Me; Et) of the *t*-butylcalix[4]arene monooxyanion $\mathbf{L}^-$ in acetonitrile solution, to compare the *endo* complexes (NR_4^+ inside the cone of the host) with the *exo* ones. For a given cation, we find that the complexes display structures of similar type in the gas phase and in acetonitrile solution. Intrinsically, the *endo* forms are more stable than *exo* ones, but they are less well solvated. As a result, *exo* complexes are predicted to be more stable than the *endo* ones in acetonitrile. In the gas phase and in solution, the *exo* complexes of NMe_4^+ and NEt_4^+ display interesting examples of fluctional intimate ion pairs, where the cation oscillates between the oxygen lower rim region of $\mathbf{L}^-$ and *exo* π stacking with the phenolic rings of $\mathbf{L}^-$. Based on free energy perturbation calculations, we compare *endo* NH_4^+/NMe_4^+ complexes and find that the hypothetical NH_4^+ complex is more stable in acetonitrile solution.

Key words: Calixarenes, molecular dynamics, binding selectivity, ion pairs, solvent effect, molecular recognition.

1. Introduction

Calixarenes, cyclo-oligomers of formaldehyde and *p*-substituted phenol, display an extraordinary versatility as metal binding agents [1]. The unsubstituted *p-tert*-butylcalix[4]arene anion $\mathbf{L}^-$ (chart I) has been shown to form neutral complexes with M^+ cations, where M^+ can be alkali [2], or ammonium cations [3]. In a recent publication we addressed the question of the *endo*/*exo* nature of the complex, i.e. whether M^+ sits as a guest inside the cone of the host, or simply forms an *exo* intimate or solvent separated ion pair with the anion [4, 5]. The alkali cations Na^+, K^+, Cs^+ were compared consistently in the gas phase, in water, chloroform and acetonitrile solutions. It was concluded that the nature of the ion pair is markedly solvent dependent. In chloroform, *endo* complexes were predicted to be more stable than the *exo* ones due to more favorable interactions with the host, whereas in acetonitrile, *exo* complexation was calculated to be preferred, because they are much better solvated [4]. In water, most complexes dissociated completely.

* Author for correspondence.

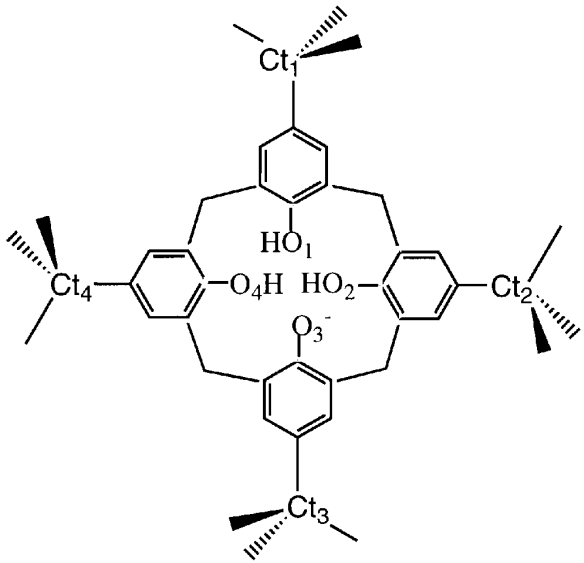

Chart I. t-Butylcalix[4]arene monooxy anion ($\mathbf{L}^-$).

These predictions have been supported by NMR investigations of the Cs^+ salt in chloroform and in acetone, an aprotic polar solvent like acetonitrile [5, 6]. In the solid state, the Cs^+ $\mathbf{L}^-$ complex is *endo* [7], whereas the Na^+ $\mathbf{L}^-$ complex is *exo*, with Na^+ 'solvated' by one MeOH and two H_2O molecules [8].

Here we extend this investigation with ammonium NR_4^+ salts of $\mathbf{L}^-$. There are indeed constrasting experimental results concerning the status of ammonium $\cdots$ calixarene interactions. The early studies of Gutsche *et al.* in acetonitrile or acetone solutions showed that calix[4]arenes interact with aliphatic amines R_3N, forming complexes that are thought to involve proton transfer from the calix[4]arene to the amine, followed by ion pairing [9]. Based on NMR results, it was suggested that the resulting complexes between R_3NH^+ and the calixarene anion are of *endo* type [9]. These results contrast with UV spectroscopy results of Görmar *et al.* concerning the interaction of more bulky cyclic amines with t-butylcalix[4]arene in acetonitrile, which have been taken as evidence for *exo* complexes between the phenolate and ammonium groups [10]. In addition to the steric fit and interactions between the calixarene cavity and R_3NH^+, the basicity of the amine and solvation effects play an important role. For instance, it was noted by Gutsche *et al.* that '*tert*-butylamine–calixarene' complexes are similar in acetone and in acetonitrile, but presumably of different nature in chloroform [9]. Based on thermodynamic and conductance studies in benzonitrile and in nitrobenzene, Danil de Namor *et al.* concluded that *tert*-butylcalix[4]arene interacts with triethylamine through hydrogen bonding or ion-pair formation [11], but the *endo*/*exo* structures cannot be assessed from these data.

For quaternary NR_4^+ salts of calixarenes, interesting solid state structures have been reported by Harrowfield *et al.* [3, 5, 12]. The NEt_4^+ cation is not included inside the cone of $\mathbf{L}^-$, which seems to prefer an acetonitrile molecule [3]. The NMe_4^+ 'salt' of the unsubstituted calix[4]arene revealed two types of cation environment: one cation sits inside the cone of a neutral host, and a second one is encapsulated in a facing pair of symmetry related calixarene monoanions [12]. The close contacts between the methyl groups of NMe_4^+ and the aromatic walls of the hosts are consistent with attractive $CH_3 - \pi$ interactions, as a possible driving force for formation of NMe_4^+ inclusion complexes with calixarenes. Collet *et al.* showed that NMe_4^+ also forms very stable inclusion complexes with neutral cryptophanes in weakly polar $(CDCl_2)_2$ and in aqueous solutions [13], presumably via similar interactions. Interestingly, by comparing two cryptophanes of different size, they noticed that in water, loose association lead to a stronger binding than does a tight association [13]. There are also examples of complexation of quaternary ammonium cations in water which generally involves negatively charged hosts such as the tetraacid derivatives of cryptophanes [13], tetrasulfonated calix[4]arene [14], or the resorcinarene tetraanions [15, 16], where the solubilizing anionic groups likely contribute to the stabilization of *endo* complexes.

These results stimulated us to study *exo*/*endo* complexes of quaternary NR_4^+ complexes of $\mathbf{L}^-$ (with R = Me; Et), first in the gas phase to compare their structures and relative stabilities, and then in acetonitrile solution, to investigate the role of a polar aprotic solvent, capable of competing with the cation inclusion. For the purpose of comparison, the NH_4^+ hypothetical salts are also simulated. In fact, NH_3 may not be basic enough to deprotonate a calix[4]arene in the gas phase, nor in acetonitrile solution. On the other hand, it cannot be ruled out that the $\mathbf{L}^-$ NH_4^+ ion pair could be stabilized by enhanced host/guest interactions, compared to the $\mathbf{L}H{\cdot}NH_3$ pair. Concerning the host–guest interactions, the binding of NH_4^+ may display analogies with that of R—NH_3^+ which binds *endo* to the calix[4]arene anion with different alkyl groups R, suggesting that R is weakly involved in the cation binding, compared to the NH_3^+ anchoring group [9]. On the other hand, the interactions with the solvent should be quite different for *exo* NH_4^+ compared to these R—NH_3^+ complexes.

Computational modeling on calixarenes involves molecular mechanics studies on their conformational properties *in vacuo* [17] and molecular dynamics studies in solution. Grootenhuis *et al.* investigated their acid-base and structural properties [18]. Simulations on alkali cation complexes involve studies on calixspherands in water [19], calix[4]tetraamides in water [20] and in acetonitrile [21], on calix[4]crowns and bis-crowns in water, methanol, acetonitrile and chloroform [22, 23]. Alkaline earth and UO_2^{2+} complexes of the calix[5]arene^{5-} and calix[6]arene^{6-} anions [24] and of a calix[4]tetraamide [25] have also been simulated in water. Recently, the interfacial behaviour of several calix[4]arenes at a liquid-liquid interface has been simulated [3, 23, 26]. Schneider *et al.* reported modeling studies on ammonium binding by resorcinarenes [15] but, to our knowledge,

no theoretical study on ammonium complexes of calixarenes has been reported so far in solution.

2. Methods

We used the AMBER software [27] for molecular mechanics and molecular dynamics simulations, with the following representation of the potential energy:

$$E_T = \Sigma_{\text{bonds}} K_r (r - r_{\text{eq}})^2 + \Sigma_{\text{angles}} K_\theta (\theta - \theta_{\text{eq}})^2 + \Sigma_{\text{dihedrals}} V_n (1 + \cos n\phi) + \Sigma_{i<j} (\epsilon_{ij} (R^*_{ij}/R_{ij})^{12} - 2\epsilon_{ij} (R^*_{ij}/R_{ij})^6 + q_i q_j / R_{ij})$$

The $\mathbf{L}^-$ host and the NR_4^+ ions are represented in the all-atom model. The bonds and bond angles are treated as harmonic springs, and a torsional term is associated with the dihedral angles. The interactions between atoms separated by at least three bonds are described by a pairwise additive 1-6-12 potential. The host is built from one phenolate and three phenol residues, connected by explicit CH_2 groups. Force field parameters for $\mathbf{L}^-$ are from Grootenhuis *et al.* [18] and the same as in Refs. [4, 5]. The cation parameters are taken from the free energy study of Rao and Singh [28, 29]. For the acetonitrile solvent, we use the OPLS model, where the methyl group is represented in the united atom approximation [30].

The solvent box is a 'cube' box of 28–30 Å length, containing 504–675 acetonitrile molecules (see Table II), with periodic boundary conditions. In solution, all X—H bonds of $\mathbf{L}^-$ and of NR_4^+ (X = C; O; N) have been constrained to constant values with SHAKE, in conjunction with a time step of 2 fs. In the gas phase, the time step was 1 fs, without SHAKE.

After 1000 steps of conjugate gradient energy minimization, the MD simulations were run for 200 ps at 300 K in acetonitrile at constant volume using the Verlet algorithm, starting with random velocities. A residue based cut-off of 10 Å was used for non-bonded interactions, taking the ion pair as a single residue. The temperature was controlled by velocity scaling in the gas phase, and by coupling to a thermal bath in solution.

The 'FEP' (free energy perturbation) calculations on NH_4^+/NMe_4^+ complexation were performed with the windowing technique, changing the parameters of NR_4^+ linearly with λ: $V_\lambda = \lambda \cdot V_{NH_4^+} + (1 - \lambda) \cdot V_{NMe_4^+}$. For the free or complexed states, the mutation was performed stepwise, with electrostatic/van der Waals decoupling, following the procedure of Rao and Singh [28, 29]: $\Delta G = \Delta G_{\text{el}} + \Delta G_{\text{vdW}}$. The ΔG_{el} contribution corresponds to mutation of the atomic charges on NR_4^+ and the ΔG_{vdW} term corresponds to mutation of the parameters R^* and ϵ. Each step was split into 21 windows. At each window, 1 ps of equilibration was followed by 1 ps of data collection, and the change of free energy ΔG was averaged from the forward and backward cumulated values.

Table I. $NR_4^+\mathbf{L}^-$ *exo/endo* complexes in the gas phase. Average energies (kcal/mol) and structural parameters.

	NH_4^+		NMe_4^+		NEt_4^+	
	endo	*exo*	*endo*	*exo*	*endo*	*exo*
Average energy components[a]						
E_{L^-}	0.0	−6.6	0.0	−3.9	0.0	−3.9
	(−111.9)		(−116.3)		(−117.2)	
$E_{NR_4^+\cdots L^-}$	0.0	9.1	0.0	12.1	0.0	6.7
	(−130.2)		(−88.2)		(−72.7)	
Average structural parameters[b]						
$O_1\cdots O_3$	3.0 ± 0.1	3.6 ± 0.4	3.7 ± 0.1	3.7 ± 0.3	3.7 ± 0.2	3.7 ± 0.3
$O_2\cdots O_4$	4.5 ± 0.1	4.0 ± 0.4	3.8 ± 0.1	4.0 ± 0.3	3.7 ± 0.2	4.0 ± 0.2
$C_{t1}\cdots C_{t3}$	9.8 ± 0.2	8.7 ± 0.8	8.7 ± 0.2	8.6 ± 0.5	8.8 ± 0.3	8.5 ± 0.5
$C_{t2}\cdots C_{t4}$	6.5 ± 0.2	7.7 ± 0.9	8.5 ± 0.2	7.8 ± 0.6	8.8 ± 0.3	7.9 ± 0.5
$N\cdots\langle O\rangle$[c]	2.7 ± 0.1	2.9 ± 0.2	4.9 ± 0.1	5.5 ± 0.8	5.8 ± 0.2	5.8 ± 0.6
$\omega 13$[d]	70 ± 7	102 ± 22	103 ± 5	106 ± 13	99 ± 10	108 ±13
$\omega 24$[d]	153 ± 5	125 ± 20	109 ± 4	124 ± 13	101 ± 9	122 ± 12

[a] kcal/mol. E_{L^-} is the energy of $\mathbf{L}^-$ within the complex and $E_{NR_4^+\cdots L^-}$ are the interaction energy between $\mathbf{L}^-$ and NR_4^+. Energies are given with respect to the *endo* complex (total values in parentheses).

[b] Average crossed $O\cdots O$ and $C_t\cdots C_t$ distances (Å). See Chart I for atom labels.

[c] Average altitude of the N atom of NR_4^+, defined by the distance between the N atom and the center of mass $\langle O\rangle$ of the four phenolic oxygens.

[d] Average angle between the planes of opposed aromatic rings.

The trajectories were saved every 0.2 ps. and analyzed with the MDS and DRAW software [31]. The average potential energy and its components are reported in Tables I and II.

3. Results

In all cases, the *endo* complexes remained *endo* while the *exo* cations remained as intimate ion pairs with $\mathbf{L}^-$ but displayed in same cases significant fluctional character. In the gas phase as in solution, for all complexes, the hydrogen bond network at the lower rim is such that the O^- oxygen is hydrogen bonded to one adjacent proton only, as in the free host [4, 5]. Simulations starting with O^- acting as a double proton acceptor converged immediately to that structure for the free and complexed host. The *t*-butyl groups rotate in most *endo* or *exo* complexes. The only exception concerns the *endo* NEt_4^+ complex, where this rotation is prevented by the guest.

In the following we focus mostly on energy and structural features related to the $\mathbf{L}^-\ldots NR_4^+$ interactions.

Table II. $NR_4^+L^-$ *exo/endo* complexes in acetonitrile. Average energies (kcal/mol) and structural parameters.

	NH_4^+		NMe_4^+		NEt_4^+	
	endo	*exo*	*endo*	*exo*	*endo*	*exo*
$Nb_{(MeCN)}$ [a]	509	504	516	520	553	675
Average energy components[b]						
E_L^-	0.0	−11.0	0.0	−1.1	0.0	−8.2
	(−104.6)		(−115.1)		(−110.6)	
$E_{NR_4^+\cdots L^-}$	0.0	11.1	0.0	14.3	0.0	7.7
	(−126.6)		(−84.3)		(−73.4)	
$E_{L^-\cdots Solv}$	0.0	1.3	0.0	3.7	0.0	2.8
	(−76.8)		(−74.0)		(−81.8)	
$E_{NR_4^+\cdots Solv}$	0.0	−23.8	0.0	−18.6	0.0	−13.4
	(−29.6)		(−25.4)		(−31.6)	
Average structural parameters[c]						
$O_1\cdots O_3$	4.4 ±0.2	3.7 ± 0.3	3.7 ± 0.2	3.7 ± 0.3	3.6 ± 0.3	3.7 ± 0.2
$O_2\cdots O_4$	2.9 ± 0.2	3.9 ± 0.3	3.8 ± 0.1	3.9 ± 0.2	3.9 ± 0.2	3.9 ± 0.2
$C_{t1}\cdots C_{t3}$	7.1 ± 0.3	8.5 ± 0.6	8.7 ± 0.2	8.6 ± 0.5	8.9 ± 0.3	8.5 ± 0.5
$C_{t2}\cdots C_{t4}$	10.2 ± 0.3	8.1 ± 0.5	8.6 ± 0.2	8.1 ± 0.5	8.6 ± 0.4	8.1 ± 0.5
$N\cdots\langle O\rangle$	2.8 ± 0.2	2.9 ± 0.2	5.1 ± 0.2	5.1 ± 1.0	6.1 ± 0.3	6.3 ± 1.1
$\omega 13$	140 ± 6	106 ± 16	104 ± 6	105 ± 14	95 ± 9	107 ±13
$\omega 24$	54 ± 13	117 ± 13	107 ± 5	118 ± 12	107 ± 9	117 ± 11

[a] Number of solvent molecules in the simulated box.
[b] Average energy of $\mathbf{L}^-$ and interaction energies between NR_4^+ and $\mathbf{L}^-$, between $\mathbf{L}^-$ and the solvent and between the solvent and NR_4^+. Fluctuations are about 5 kcal/mol for $E_{\mathbf{L}^-}$ and $E_{NR_4^+\cdots\mathbf{L}^-}$, and 9 kcal/mol for $E_{L^-\cdots Solv}$ and $E_{NR_4^+\cdots Solv}$. The 'intrinsic' energy of the complex is $E_{\mathbf{L}^-} + E_{NR_4^+\cdots\mathbf{L}^-}$. Its total interaction energy with acetonitrile is $E_{\mathbf{L}^-\cdots Solv} + E_{NR_4^+\cdots Solv}$.
[c] See definitions in Table I.

3.1. THE $NR_4^+L^-$ SALTS IN THE GAS PHASE

Cumulated views of the trajectories, obtained after removal of the total translation and rotation motions, are represented in Figure 1. The average energies of $\mathbf{L}^-$ (E_{L^-}) and cation-ligand interaction energy ($E_{M^+\ldots L^-}$) are reported in Table I. For a given cation, comparison of the *exo*/*endo* complexes indicates a preference for *endo* structures, as a result from the balance of $E_{M^+\ldots L^-}$ (which favours *endo* complexes), and of E_{L^-} (which favours the *exo* complexes).

The $E_{M^+\ldots L^-}$ interaction energies are larger for NH_4^+, than for NMe_4^+ and NEt_4^+ (Δ = 0, 42 and 51 kcal/mol respectively in the *endo* series; Δ = 0, 45 and 48 kcal/mol in the *exo* series). The $\mathbf{L}^-$ host itself has within a few kcal/mol the same energy, excepted in the NH_4^+ *endo* complex, where it is least stable (Table I).

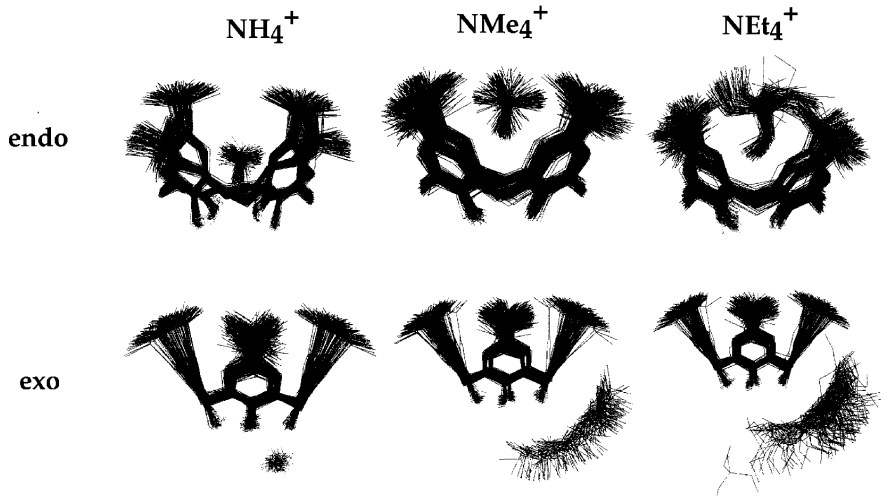

Figure 1. The $NR_4^+\mathbf{L}^-$ *endo* and *exo* complexes simulated *in vacuo.* Cumulated views after 250 ps (Orthogonal representations; hydrogen atoms are not shown, excepted on NH_4^+).

A further dissection of $E_{M^+\cdots L^-}$ into the energy contribution of the three phenolic and of the one phenolate residues shows first, as expected, that the latter brings the largest contribution, which is larger for *exo* than for *endo* complexes (76, 80 and 83% respectively for the NH_4^+, NMe_4^+, and NEt_4^+ *endo* , and 83, 98 and 92% respectively for the complexes *exo*). Second, the average contribution of the three phenolic fragments, also smaller, differs from one fragment to the other, indicating a non-symmetrical position of the cation with respect to these fragments.

For the *endo* complexes, the altitude of the $N_{NR_4^+}$ atom in the cone increases as expected from NH_4^+ (2.4 ± 0.4) to NMe_4^+ (4.8 ± 0.1) and NEt_4^+ (5.4 ± 0.6 Å) and the N atom is roughly equidistant from the four phenolic oxygens. The NH_4^+ and NMe_4^+ guests rotate inside the cone, pointing their N—H or N—Me bonds either down to the center $\langle O \rangle$ of the phenolic oxygens, or to the aromatic residues. The NEt_4^+ guest is comparatively more rigid, pointing always the same N—CH_2CH_3 branch to the $\langle O \rangle$ center along the C_4 symmetry axis (Figure 1).

In the *exo* complexes the cation sits away from the 'C_4 symmetry axis' (Figure 1). NH_4^+ interacts strongly with the phenolic O^- oxygen, making two short N$\cdots$O contacts (2.82 and 2.96 Å) and two long ones (3.66 and 3.90 Å). The NMe_4^+ and NEt_4^+ cations which have weaker interactions than NH_4^+ with $\mathbf{L}^-$ are much more mobile and oscillate between two positions: the O^- site at the lower rim, and a π-facial *exo* interaction with the phenolate ring (Figure 1). Thus, final snapshots obtained after 200 ps of simulation might be misleading, as they mask this versatility of this intimate ion pair.

Another structural parameter of interest concerns the shape and (a)symmetry of the cone, defined by the crossed distances $C_t \cdots C_t$ between opposed central t-

butyl carbons at the upper rim and O···O distances at the lower rim. These average parameters and the average ω_{13} and ω_{24} angles between the planes of opposite aromatic rings are reported in Table I. They make clear that in none of the complexes the cone is on the average or instantaneously of C_4v symmetry. This is not due to the fact that the guests have a C_3-type symmetry, since the cone is somewhat less asymmetrical in the *endo* than in the *exo* complexes. The average $O_{(H)1}\cdots O_{(H)3}$ distance is smaller than $O_{(-)2}\cdots O_{(H)4}$ (by about 0.1 Å for *endo* complexes and 0.3 Å for *exo* complexes). The corresponding $C_{t1}\cdots C_{t3}$ and $C_{t2}\cdots C_{t4}$ distances follow the opposite trend, as a result of the mechanical top–bottom coupling [21]. Taking the example of the NMe_4^+ complex to illustrate dynamic features, we find that the motions have an amplitude of about 0.8 Å for $C_t\cdots C_t$ and 0.4 Å for O···O distances, and are anticorrelated. The correlation coefficient χ is most negative for *exo* complexes, and about the same for $C_{t1}\cdots C_{t3}/C_{t2}\cdots C_{t4}$ ($\chi_{\text{top}} = -0.92$) as for $O_1\cdots O_3/O_2\cdots C_4$ ($\chi_{\text{bottom}} = -0.91$), indicative of coupled top–bottom motions. This contrasts with *endo* complexes, where the NMe_4^+ host perturbs the motions of the host which become less correlated at the 'top' ($\chi_{\text{top}} = -0.27$) than at the 'bottom' ($\chi_{\text{bottom}} = -0.62$). The cone of the NH_4^+ complex is the most asymmetrical one (Table I).

3.2. THE CALIX$^-$ NR_4^+ COMPLEXES IN ACETONITRILE

The solvation of the free $\mathbf{L}^-$ calixarene has been described in Refs. [4, 5]. One important feature is the filling of the cone by two solvent molecules, oriented with their methyl groups pointing toward the phenolic oxygens, as governed by dipole-dipole interactions between MeCN and the host. With the exception of NH_4^+ *endo*, all complexes behave in acetonitrile (Figures 2 and 3) as *in vacuo*.

In particular, the altitude of $N_{NR_4^+}$ *endo* is within 0.2 Å the same in acetonitrile as in vacuo. The *endo* NH_4^+ and NMe_4^+ cations undergo rapid rotation motions, while NEt_4^+ is anchored via one NEt chain inside the cone. The *exo* NH_4^+ complex remains bound at the lower rim to the phenolate O^- oxygen, while the two other cations exchange as in the gas phase between this O^- lower rim and *exo* π-facial interactions with the phenolate ring. Thus, despite these motions and the polarity of the solvent, none of the *exo* complex fully dissociates.

As in the gas phase, *endo* cations interact better than the *exo* ones with $\mathbf{L}^-$ (by 11, 14 and 8 ± kcal/mol, respectively for NH_4^+, NMe_4^+ and NEt_4^+) while $\mathbf{L}^-$ is more stable in *exo* than in *endo* complexes (by 11, 1 and 8 kcal/mol, respectively). Taking into account these two components leads to a comparable intrinsic stability for *endo*/*exo* complexes of NH_4^+ and NEt_4^+, and to a larger intrinsic stability of NMe_4^+ *endo* compared to *exo* (Δ = 13 kcal/mol). On the other hand, all *exo* complexes are solvated much better than the *endo* ones (by 22, 15 and 11 kcal/mol respectively for NH_4^+, NMe_4^+ and NEt_4^+, mostly due to the contribution of NR_4^+; see Table II). Thus, for all cations, the difference in solvation energies is larger

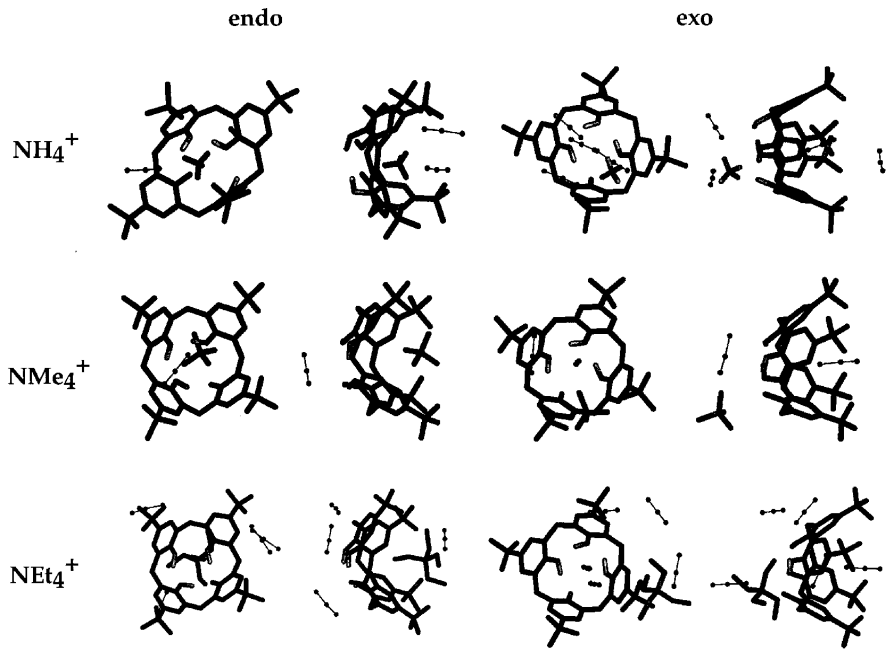

Figure 2. The $NR_4^+L^-$ *endo* and *exo* complexes in acetonitrile. Snapshots after 200 ps of MD, including selected solvent molecules. Orthogonal views.

than, or comparable to the *endo*/*exo* energy difference of intrinsic stabilities. The net balance is largest for NH_4^+ (Δ = 11 kcal/mol), which should be more stable *exo* in acetonitrile solution. For the NMe_4^+ complex, both contributions are comparable, and the *endo*/*exo* forms should be of similar energy in acetonitrile. For the NEt_4^+ complex, the *exo* binding would be slightly preferred over the *endo* binding, due to the solvent contribution.

As expected, all cations are coordinated to MeCN molecules by their negatively charged N atom, and *exo* cations are more solvated than the *exo* ones. The radial distribution functions (rdf) of N_{MeCN} around the N atom of NR_4^+ were calculated (Figure 4) to obtain the coordination number of NR_4^+, by integrating the first peak. The coordination numbers are 4.5, 3.5, and 2.9, respectively for *exo* NH_4^+, NMe_4^+ and NEt_4^+ cations, and 1.9, 1.9, and 3.5, respectively for the *endo* cations. Thus, the coordination number does not simply increase with the size of the cation, as we found with alkali cation *exo* complexes [4, 5], because of the steric hindrance of the Me and Et groups in NR_4^+. A second significant solvent stabilization of the *exo* complexes is provided by one MeCN molecule which sits inside the cone, with its methyl group pointing to the phenolic oxygens, as in the free $\mathbf{L}^-$ host [4, 5].

As in vacuo, the cone is somewhat asymmetrical (Table II) and displays the same type of asymmetry. In the NH_4^+ **endo** complex, which has the most 'rectangular' C_{2v}-like cone, the cation sits very deeply inside the cone, and is coordinated to

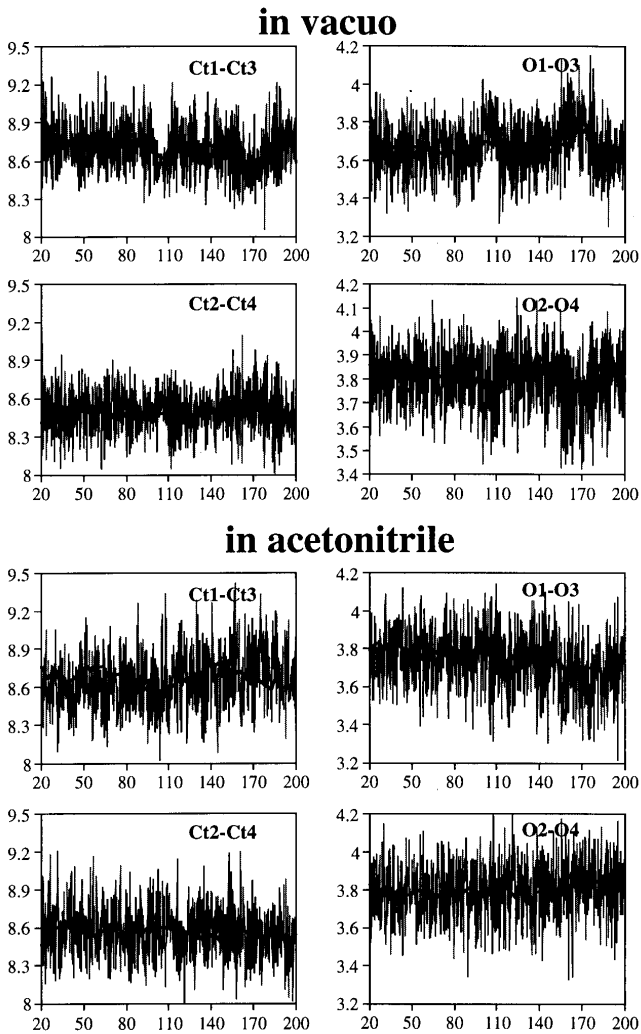

Figure 3. The *endo* $NMe_4^+\mathbf{L}^-$ complex in the gas phase and in acetonitrile: Crossed $C_t \cdots C_t$ and O···O distances as a function of time.

two MeCN molecules which contribute to rigidify the cone (Figure 2). The average $C_{t1} \cdots C_{t3}$ distance is about 3 Å larger than the $C_{t2} \cdots C_{t4}$ one, as in the gas phase. For all complexes, the time dependent oscillations of the cone shape have about the same amplitude as the gas phase (Figure 3), but are somewhat less correlated. For instance with the NMe_4^+ complex *exo*, the correlation coefficients χ_{top} and χ_{bottom} (respectively -0.78 and -0.83) are smaller than in the gas phase (respectively -0.92 and -0.91) due to the fact that the cone is filled by one MeCN guest solvent molecule. For the *endo* complex, χ_{top} and χ_{bottom} are smaller (respectively -0.36 and -0.68), because of the NMe_4^+ guest sitting inside the cone.

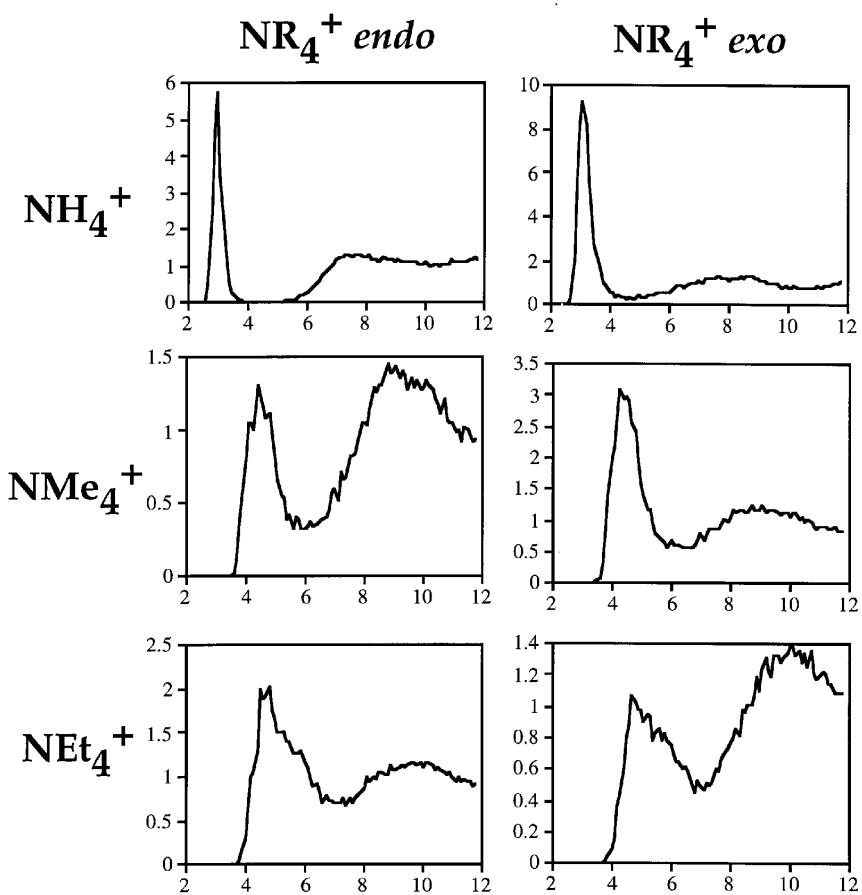

Figure 4. The $NR_4^+\mathbf{L}^-$ complexes *exo* and *endo*: $NR_4^+ \cdots N_{MeCN}$ *rdf*'s. in acetonitrile.

3.3. CALCULATED RELATIVE BINDING SELECTIVITIES UPON COMPLEXATION: FREE ENERGY SIMULATIONS IN THE GAS PHASE AND IN ACETONITRILE SOLUTION

Free energy perturbation calculations have been reported to compare the solvation of ammonium ions in water [28], hydrazine and carbon tetrachloride [29] solutions, but their complexes with synthetic hosts have not been simulated so far by such techniques. Here, we use a thermodynamic cycle to calculate the NH_4^+/NMe_4^+ binding selectivity ΔG_c. The experimental value $\Delta G_c = \Delta G_1 - \Delta G_2$ is obtained computationally via the 'alchemical route' [32, 33] as $\Delta G_c = \Delta G_3 - \Delta G_4$.

To our knowledge, no experimental values have been reported for the ammonium salts in acetonitrile. We decided to consider only the *endo* complexes, because the fluctional character of some of the *exo* ones would cause sampling problems during

Table III. Relative free energies of mutation (kcal/mol) of NH_4^+ to NMe_4^+ uncomplexed and complexed by L^-.

Mutation	ΔG_{ele}	ΔG_{vdW}	Total	Exp.[a]
$NH_4^+ \rightarrow NMe_4^+$ *in water*	0.6	29.2	29.8	31.7
$NH_4^+ \rightarrow NMe_4^+$ *in acetonitrile*	0.2	30.4	30.6	–
$NH_4^+/L^- \rightarrow NMe_4^+$ *in acetonitrile*	0.2	36.3	36.5	–

[a] Taken from Rao and Singh [28].

the FEP calculation. On the other hand, *exo* NR_4^+ cations are markedly solvated, and should behave more like the free ones.

$$\begin{array}{ccc} \mathbf{L}^- + NH_4^+ & \xrightarrow[\Delta G_1]{} & \mathbf{L}NH_4 \\ {\scriptstyle \Delta G_3}\downarrow & & \downarrow{\scriptstyle \Delta G_4} \\ \mathbf{L}^- + NMe_4^+ & \xrightarrow[\Delta G_2]{} & \mathbf{L}Me_4 \end{array}$$

The results are reported in Table III for the *endo* complexes. For the free cations, we first checked that the NH_4^+/NMe_4^+ difference in solvation free energies ΔG_3 calculated in water is the same as the one reported by Rao and Singh (29.8 kcal/mol) [28], and close to the experimental value of 31.7 kcal/mol. In acetonitrile, we calculate a ΔG_3 value of 30.6 kcal/mol, indicating that NH_4^+ is also best solvated, mostly due to the ΔG_{vdW} energy component. To our knowledge, there are no related experimental data. For the ammonium complexes, the change in free energy ΔG_4 (36.5 kcal/mol) indicates that NH_4^+ also interacts best with $\mathbf{L}^-$ and with the solvent, as seen above from the energy component analysis (Table II). This leads to $\Delta G_c = \Delta G_3 - \Delta G_4 = -6.0$ kcal/mol, which means that the *endo* NMe_4^+ complex is less stable than the *endo* NH_4^+ complex in acetonitrile solution.

4. Discussion and Conclusion

Molecular dynamics and free energy perturbation simulations have been performed on the NR_4^+ ammonium salts (R = H; Me; Et) of *t*-butyl-calix[4]arene monooxyanion $\mathbf{L}^-$ in the gas phase and in acetonitrile solution. Structural and energy characteristics were analyzed by a systematic comparison of *exo* 'exclusive' and *endo* 'inclusive' complexes.

4.1. LOCATION OF THE CATION IN THE COMPLEX WITH CALIX$^-$: *endo* OR *exo*? INTRINSIC STABILITIES VERSUS SOLVATION EFFECTS

In our MD simulations, no dissociation of the $\mathbf{L}^-$ NR_4^+ ion pair takes place in the gas phase or in acetonitrile solution. The relatively long lifetime of the intimate ion pairs (>200 ps) indicates that the acetonitrile solvent is not a strong competitor with such ion pairing. This contrasts with our previous results in water, where the *exo* Cs^+ cation dissociates from $\mathbf{L}^-$ in less than 3 ps, while the *endo* Cs^+ decomplexes in less than 100 ps [4]. In acetonitrile solution, the simulations limited to 200 ps because of computer time limitations, do not show a dynamic exchange between *endo* and *exo* $\mathbf{L}^-$ complexes. They are thus expected to display only weak conductivities in acetonitrile or in less dissociating solvents like benzonitrile or nitrobenzene [11]. For the NH_4^+ $\mathbf{L}^-$ hypothetical complex, a weak conductivity might result also from the proton transfer to $\mathbf{L}^-$, to form the NH_3. **LH** complex, where presumably NH_3 sits inside the cone of **LH**.

The energy component analysis (Table II) indicates that the status of this ion pair depends on two opposite components: host–guest interactions favour the *endo* form, while solvation favours the *exo* form. At a quantitative level, force field limitations cannot be precluded as we used a 1-6-12 potential for non-covalent interactions, without many-body and polarization contributions [34]. Electrostatics has been shown, however, to provide a predictive tool for cation–π interactions [35]. Based on our results, we would conclude that in acetonitrile solution, none of the NR_4^+ cations considered here displays a clear preference for *endo* complexation. The energy balance in favour of *exo* binding is the largest for NH_4^+, compared to the other cations. For NMe_4^+, the situation is less clear. It is likely that an explicit account of polarization effects would reinforce the intrinsic preference for *endo* binding, as calculated for the Cs^+ complex [4], but this requires additional more sophisticated calculations and force field developments. For the NEt_4^+ cation, the balance is more clearly in favour of *exo* binding than for NMe_4^+.

A number of related structural results have been reported. The tetra-sulfonato-calix[4]arene binds quaternary ammonium cations in water ($\log K_s > 4$) [14] presumably as *endo* complexes, as in the solid state structure of the choline [14] or NMe_4^+ [37] complexes. However, this cannot be compared with $\mathbf{L}^-$ complexes, where the upper rim of the cone is substituted by *t*-butyl instead of $-SO_3^-$ groups. The latter create an electrostatic field which favours *endo* complexation. The solid state structures of the NEt_4^+ [3] and NBu_4^+ [5] $\mathbf{L}^-$ complexes show that the cone of $\mathbf{L}^-$ is not filled by the cation, but by one MeCN molecule. The NEt_4^+ cation forms a column with $\mathbf{L}^-$, sitting at the lower rim of one $\mathbf{L}^-$ and on the top of the MeCN molecule which sits in the cone of another equivalent $\mathbf{L}^-$. In polar solvents, there is no clear evidence of *endo* ammonium complexes of $\mathbf{L}^-$. The ^{1}H NMR data with NMe_4^+ in DMSO are indicative of interactions between the cation and $\mathbf{L}^-$, with a rapid site exchange, but no firm conclusion could be drawn on the nature of the interactions [3]. Indeed, the upfield shifts of methyl resonances of NMe_4^+,

comparable with $\mathbf{L}^-$ as with the calix[4]arene anion, do not exclude *endo* complex formation, but are not consistent either with *endo* complex being the dominant species. In acetone, no shift was found for NEt_4^+. Thus, these experimental and our calculated results converge to a similar view, where the NR_4^+ complexes of $\mathbf{L}^-$ do not display a clear preference for being of inclusive type in polar solvents like acetonitrile or acetone. It is also clear from our previous study [4] that, as the polarity of the solvent increases, *exo* 'complexation' (or even full ion pair dissociation) is favoured. Conversely, in the gas phase or in a weakly polar solvent like chloroform, *endo* complexation with formation of host–guest adducts is favoured.

Concerning the relevance of solid state structures for the solution state, it has been emphasized that "a species depositing from a given solution may not necessarily be that which is the most abundant in solution" [36]. Based on our simulations, it is also important to note the differences in cation environment in the solid state, compared to the solution. In the case of the *endo* NMe_4^+ complex of the calix[4]arene, in the crystal, the cation is encapsulated inside the cone, and shielded from the 'solvent' (water molecules) [12]. In the simulated acetonitrile solution of the *endo* NMe_4^+ $\mathbf{L}^-$ complex, the cation, although surrounded by the four t-butyl groups, is solvated by two MeCN molecules. A second example is provided by the *exo* NEt_4^+ $\mathbf{L}^-$ adduct where, in the crystal, the cation sits on the 'fourfold' symmetry axis of the cone, in contact with the phenolate oxygens of $\mathbf{L}^-$ on one side, and with the t-butyl groups of another $\mathbf{L}^-$ and a MeCN molecule on the other side [3]. When simulated in solution, NEt_4^+ fluctuates between the lower rim region of $\mathbf{L}^-$ and a π-facial stacking position over the phenolate ring, and is coordinated to 3–4 MeCN molecules, never reaching the upper rim region of the host. As the *endo*/*exo* nature of the complex is not only determined by the NR_4^+–host interactions, but also from the environment, it is stressed that differences in short range and in long range interactions between the cation and its surrounding may modulate the nature of the complex.

4.2. On the NH_4^+/NMe_4^+ *endo* binding selectivity

Based on free energy perturbation calculations, we have compared the binding of NH_4^+ with the simplest quaternary ammonium NMe_4^+ ion. As found for alkali cations, the smallest ion is best solvated in its free state, and interacts best with the negatively charged host. The binding selectivity in acetonitrile results therefore from the compensation between these two components. We calculate that NH_4^+ would bind better than NMe_4^+ to $\mathbf{L}^-$, if *endo* complexation takes place. For *exo* salts, no FEP calculation was undertaken, as it is clear from the energy component analysis (Table II) that NH_4^+ interacts better also with $\mathbf{L}^-$ and with the solvent than does NMe_4^+. To our knowledge, no related data are available. We hope that this study will stimulate further experimental investigations, including related basicity measurements [11, 38].

Beyond the $\mathbf{L}^{-}\ NR_4^+$ system studied here, this solvent and environment dependent nature of the ion pair between putative hosts and guests may be of importance for other questions such as acetylcholine complexation in biological systems, and binding of ammonium cations to electron-rich π systems [39–44].

Acknowledgements

The authors are grateful to the CNRS for allocation of computer time on IDRIS, to E. Engler and A. Varnek for assistance, and to Prof. J. Harrowfield for stimulating discussions. FF is grateful to EEC for a grant (CHRX-CT94-0484 contract).

References

1. V. Böhmer: *Angew. Chem. Int. Ed. Engl.* **34**, 713 (1995). J. Vicens, Z. Asfari and J.M. Harrowfield: *Calixarenes 50th Anniversary: Commemorative Issue.* Kluwer Academic Publishers, Dordrecht, (1995). J. Vicens and V. Böhmer: *Calixarenes: a Versatile Class of Macrocyclic Compounds.* Kluwer Academic Publishers, Dordrecht (1991).
2. R.M. Izatt, J.D. Lamb, R.T. Hawkins, P.R. Brown, S.R. Izatt and J.J. Christensen: *J. Am. Chem. Soc.* **105**, 1782 (1983). H. Goldman, W. Vogt, E. Paulus and V. Böhmer: *J. Am. Chem. Soc.* **110**, 6811 (1988).
3. J.M. Harrowfield, M.I. Ogden, W.R. Richmond, B.W. Skelton and A. White, *J. Chem. Soc. Perk. Trans 2*, 2183 (1993).
4. A. Varnek, C. Sirlin and G. Wipff: In *Crystallography of Supramolecular Compounds.* (ed. G. Tsoucaris), p. 67. Kluwer Academic Publishers, Dordrecht (1995).
5. R. Abidi, M.V. Baker, J.M. Harrowfield, D.S.-C. Ho, W.R. Richmond, B.W. Skelton, A.H. White, A. Varnek and G. Wipff: *Inorg. Chim. Acta* **246**, 275 (1996).
6. R. Assmus, V. Böhmer, J. Harrowfield, M.I. Ogden, W.R. Richmond, B.W. Skelton and A.H. White, *J. Chem. Soc. Dalton Trans.* 2427 (1993).
7. J.M. Harrowfield, M.I. Ogden, W.R. Richmond and A.H. White: *J. Chem. Soc. Chem. Commun.* 1159 (1991).
8. F. Hamada, K.D. Robinson, G.W. Orr and J.L. Atwood: *Supramol. Chem.* **2**, 19 (1993).
9. L.J. Bauer and C.D. Gutsche: *J. Am. Chem. Soc.* **107**, 6063 (1985). C.D. Gutsche, M. Iqbal and I. Alam: *J. Am. Chem. Soc.* **109**, 4314 (1987). See also C.D. Gutsche: *Calixarenes*, J.F. Stoddart (ed.), Royal Society of Chemistry, Cambridge, U.K., pp. 164–167 (1989)
10. G. Görmar, K. Seiffarth, M. Schulz and C.L. Chachimbombo: *J. Prakt. Chem.* **333**, 475 (1991).
11. A.F. Danil de Namor, J. Wang, I. Gomez Orellano, F.J. Sueros Velarde and D.A. Pacheco Tanaka: *J. Incl. Phenom.* **19**, 371 (1994). A.F. Danil de Namor, P.M. Blackett, M.T. Garrido Pardo, D.A. Pacheco Tanaka and F.J. Sueros Vellarde, M.C. Cabaleiro: *Pure Appl. Chem.* **65**, 415 (1993). A.F. Danil de Namor, M.T. Garrido Pardo, D.A. Pacheco Tanaka, F.J. Sueros Velarde, J.D. Cardenas Garcia, M.C. Cabaleiro and J.M.A. Al-Rawi: *J. Chem. Soc. Faraday Trans.* **89**, 2727 (1993).
12. J.M. Harrowfield, W.R. Richmond, A.N. Sobolev and A.H. White: *J. Chem. Soc. Perkin Trans 2*, 5 (1994).
13. L. Garel, B. Lozach, J.-P. Dutasta and A. Collet: *J. Am. Chem. Soc.* **115**, 11652 (1993). See also A. Collet: *Cryptophanes*: In *Comprehensive Supramolecular Chemistry*, (eds. J.L. Atwood, J.E.D. Davies, D.D. McNicol and F. Vögtle), p. 325. Pergamon, **2**, (1996) and references cited therein.
14. J.-M. Lehn, R. Meric, J.-P. Vigneron, M. Cesario, J. Guilhem, C. Pascard, Z.Asfari and J. Vicens: *Supramol. Chem.* **5**, 97 (1995).
15. H.-J. Schneider and U. Schneider: *J. Org. Chem.* **52**, 1613 (1987); *J. Incl. Phenom.* **19**, 67 (1994). H.-J. Schneider, D. Güttes and U. Schneider: *J. Am. Chem. Soc.* **110**, 6449 (1988); *Angew. Chem. Int. Ed. Engl.* **25**, 647 (1986). U. Schneider and H.-J. Schneider: *Chem. Ber.* **127**, 2455 (1994).
16. H.-J. Schneider: *Angew. Chem. Int. Ed. Engl.* **30**, 1417 (1991). See also K. Kobayashi, Y. Asakawa and Y. Aoyama: *Supramol. Chem.* **2**, 133 (1993).

17. J. Royer, F. Bayard and C. Decoret, *J. Chim. Phys.* **87**, 1695 (1990). X. de Mendoza, P. Prados, N. Campillo, P.M. Nieto, C. Sachez, J.-P. Fayet, M.C. Vertut, C. Jaime and J. Elguero: *Recl. Trav. Chim. Pays-Bas* **112**, 367 (1993). T. Harada and S. Shinkai: *J. Chem. Soc. Perkin Trans. 2* 2231 (1995). K. Lipkowitz and G. Pearl: *J. Org. Chem.* **58**, 6729 (1993). L.C. Groenen, J.-D. van Loon, W. Verboom, S. Harkema, A. Casnati, R. Ungaro, A. Pochini, F. Ugozzoli and D.N. Reinhoudt: *J. Am. Chem. Soc.* **113**, 2385 (1991). I. Thondorf, G. Hillig, W. Brandt, J. Brenn,d A. Barth and V. Böhmer: *J. Chem. Soc., Perkin Trans. 2*, 2259 (1994).
18. P.D.J. Grootenhuis, P.A. Kollman, L.C. Groenen, D.N. Reinhoudt, G.J. van Hummel, F. Ugozzoli, G.D. Andreetti: *J. Am. Chem. Soc.* **112**, 4165 (1990).
19. S. Miyamoto and P.A. Kollman: *J. Am. Chem. Soc.* **114**, 3668 (1992).
20. P. Guilbaud, A. Varnek and G. Wipff: *J. Am. Chem. Soc.* **115**, 8298 (1993).
21. A. Varnek and G. Wipff: *J. Phys. Chem.* **97**, 10840 (1993).
22. G. Wipff and A. Varnek: *J. Mol. Struct. THEOCHEM* **363**, 67 (1996).
23. G. Wipff and M. Lauterbach: *Supramol. Chem.* **6**, 187 (1995). M. Lauterbach and G. Wipff: *Liquid-Liquid Extraction of Alkali Cations by Calix[4]crown Ionophores: a MD FEP Study in Pure Chlorofrom and at the Water/Chloroform Interface.* In *Physical Supramolecular Chemistry*, NATO ASI series, (eds. L. Echegoyen and A. Kaifer, pp. 65–102. Kluwer, Academic Publishers, Dordrecht (1996).
24. P. Guilbaud and G. Wipff: *J. Incl. Phenom.* **16**, 169 (1993). *THEOCHEM* **366**, 55 (1996).
25. N. Muzet, G. Wipff, A. Casnati, L. Domiano, R. Ungaro and F. Ugozzoli: *J. Chem. Soc. Perk. Trans. 2*, 1065 (1996).
26. G. Wipff, E. Engler, P. Guilbaud, M. Lauterbach, L. Troxler and A. Varnek: *New J. Chem.* **20**, 403 (1996). A. Varnek and G. Wipff: *J. Comput. Chem.* **17**, 1520 (1996).
27. D.A. Pearlman, D.A. Case, J.C. Cadwell, G.L. Seibel, U.C. Singh, P. Weiner and P.A. Kollman: *AMBER4*; University of California: San Francisco (1991).
28. B.G. Rao and U.C. Singh: *J. Am. Chem. Soc.* **111**, 3125 (1989).
29. B.G. Rao and U.C. Singh: *J. Am. Chem. Soc.* **113**, 4381 (1991).
30. W.L. Jorgensen and J.M. Briggs: *Mol. Phys.* **63**, 547 (1988).
31. E. Engler and G. Wipff: *MD-DRAW. A Program for graphical representation and analysis of molecular trajectories in solution.* Université Louis Pasteur, Strasbourg (1994).
32. W.L. Jorgensen: *Acc. Chem. Res.* **22**, 184 (1989).
33. T. Straatsma and J.A. McCammon: *Annu. Rev. Phys. Chem.* **43**, 407 (1992).
34. J. Caldwell and P.A. Kollman: *J. Am. Chem. Soc.* **117**, 4177 (1995).
35. S. Mecozzi, A.P. West and D.A. Dougherty: *J. Am. Chem. Soc.* **118**, 2307 (1996).
36. J. Harrowfield, W.R. Richmond and A.N. Sobolev: *J. Incl. Phenom.* **19**, 257 (1994).
37. J. Atwood, L.J. Barbour, P.C. Junk, G.W. Orr: *Supramol. Chem.* **5**, 105(1995).
38. N.S. Isaacs: *Physical Organic Chemistry*, Longman (1987).
39. K.S. Kim, J.Y. Lee, S.J. Lee, T.-K. Ha and D.H. Kim: *J. Am. Chem. Soc.* **116**, 7399 (1994). J. Gao: *Biophys. J.* **65**, 43 (1993). P.H. Axelsen: *Isr. J. Chem.* **34**, 159 (1994).
40. P.C. Kearney, L.S. Mizoue, R.A. Kumpf, J.E. Forman, A. McCurdy and D.A. Dougherty: *J. Am. Chem. Soc.* **115**, 9907 (1993).
41. F. Diederich, W.F. van Gunsteren, T.C. Beutler and T.Z.M. Denti: *J. Phys. Chem.* **100**, 4256 (1996).
42. W.L. Jorgensen, T.B. Nguyen, E.M. Sanford, I. Chao, K.N. Houk and F. Diederich: *J. Am. Chem. Soc.* **114**, 4003 (1992).
43. K.N. Koh, K. Araki, A. Ikeda, H. Otsuka and S. Shinkai: *J. Am. Chem. Soc.* **118**, 755 (1996). S. Shinkai, K. Araki, T. Matsuda, N. Nishiyama, H. Ikeda, I. Takasu and M. Iwamoto: *J. Am. Chem. Soc.* **112**, 9053 (1990).
44. R. Meric, J.-P. Vigneron and J.-M. Lehn: *J. Chem. Soc. Chem. Commun.* 129 (1993).